Supplementary material

Zhou M, Lei L, Chen W, et al. Deep learning-based diagnosis of aortic dissection using electrocardiogram: Development, validation, and clinical implications of the AADE score. Kardiol Pol. 2024.

Appendix 1. Data collection

In this study, we conducted a detailed analysis of various variables in aortic dissection (AD) patients compared with non-AD patients. In addition to basic demographic and clinical parameters such as age, gender, height, weight, body mass index (BMI), body temperature, systolic blood pressure (SBP), and diastolic blood pressure (DBP), we also scrutinized health conditions like hypertension, diabetes, renal insufficiency, hyperlipidemia, coronary artery disease, cerebrovascular disease, respiratory system diseases, digestive system diseases, trauma or injury, as well as smoking and alcohol (individuals who have smoked continuously for more than six months and quit smoking for less than six months were classified as smokers. Drinking more than once a week was classified as alcohol use), and hospital mortality rates. Further, we included analyses of AD type, creatinine, glomerular filtration rate (eGFR), C-reactive protein (CRP), cardiac troponin (CTn), prothrombin time (PT), fibrinogen (Fbg), activated partial thromboplastin time (APTT), thrombin time (TT), and D-dimer.

The analysis of electrocardiographic (ECG) features encompassed ST-T abnormalities, ST elevation, ST depression, anterior/lateral/inferior wall ST depression, T-wave inversions, sinus tachycardia, sinus bradycardia, left ventricular hypertrophy (LVH), left atrial enlargement, left anterior fascicular block (LAFB), right bundle branch block (RBBB), ventricular premature beats (VPBs), atrial premature beats (APBs), atrial fibrillation (AF), and first-degree atrioventricular block.

All data were obtained through standardized medical examinations and laboratory tests. Demographic data and medical histories of patients were collected from medical record systems. Biochemical markers were analyzed from blood samples collected at the time of patient admission. ECG features were recorded and analyzed using standard electrocardiographic equipment following routine procedures.

Appendix 2. Model description

Our CNN model is built based on ResNet, which is denoted in figure S2. The symbols “k”, “c”, and “s” represent kernel size, channels, and stride respectively. Our model is made by stacked residual blocks. The structure of our model is as follows:

The first layer is the convolutional layer which convolves the output of the previous layer with a set of kernels to extract a set of features at different locations of the original image and obtain the representation which is called the feature maps. The second layer is the batch normalization (BN). layer which normalizes the values of different feature maps in the previous layer and followed by an activation function called RELU. The third layer is the max pooling layer which lowers the computational burden by compressing the feature map processed by previous layers. The following 16 layers are residual blocks with different channels and strides. The residual block includes two convolutional layers which followed by BN and RELU, the difference between the two convolutional layer is that the latter applies RELU after a shortcut connection. The next layer is the global average pooling layer which generates the final features and reduces the risk of overfitting by largely decreasing the number of parameters. The last layer is the softmax layer which provides the posterior probability of each class by a softmax function.

Our framework is implemented based on PyTorch and run on NVIDIA GTX 2080Ti graphics card. In our proposed CNN structure, the kernel size of each convolution is fixed to 13, the pooling size of max-pooling layer is fixed to 3 with the pooling stride fixed to 2. An effective optimization method named as Adam is adopted to achieve

efficient computing. A weighted loss function named as focal loss is adopted during the training to achieve better performance by focusing on the samples that are not easily classified. The hyperparameters of our proposed CNN are set to {4, 0.00003, 50}, which denote the batch size, learning rate, and training epoch respectively. We calculated the accuracy, sensitivity, specificity, F1 score, and area under the receiver operating characteristic curve (AUROC) to assess the performance of the models on the test dataset.

REFERENCES

1. He K, Zhang X, Ren S, et al. Deep residual learning for image recognition. 2016 IEEE Conference on Computer Vision and Pattern Recognition (CVPR). 2016: 770–778, doi: 10.1109/cvpr.2016.90.
2. Ioffe, Sergey, Christian Szegedy. Batch normalization: Accelerating deep network training by reducing internal covariate shift International conference on machine learning, 2015: 448-456.
3. Nair V, Hinton GE. Rectified linear units improve restricted boltzmann machines Proceedings of the 27th international conference on machine learning (ICML-10), 2010: 807-814.
4. Kingma DP, Ba J. Adam: A method for stochastic optimization. arXiv preprint . 2014: 1412–6980.
5. Lin TY, Goyal P, Girshick R, et al. Focal loss for dense object detection Proceedings of the IEEE international conference on computer vision, 2017: 2980-2988.

Appendix 3. Detailed diagnostic criteria for ECG abnormalities

1. ST-T abnormalities: These are typically considered significant if the ST segment displacement is ≥1mm (0.1 mV).

2. ST elevation: At the J point in at least two contiguous leads with the cut-off points: ≥0.2 mV in men or ≥0.15 mV in women in leads V2–V3 and/or ≥0.1 mV in other leads.

3. ST depression: ST depression of at least 0.05 mV at the J point, ST segment, or

minimum point in non-Q wave.

4. Anterior wall/anterolateral wall/inferior wall ST depression: ST depression noted in corresponding leads (anterior wall: V1–V4; anterolateral wall: I, aVL, V5, V6; inferior wall: II, III, aVF).

5. T-wave inversion: Inversion of T waves in at least two related leads may indicate myocardial ischemia, electrolyte imbalances, pulmonary hypertension, and more.

6. Anterior wall/anterolateral wall/inferior wall/lateral wall T-wave inversion: T wave inversion noted in corresponding leads.

7. Sinus tachycardia: Heart rate exceeding 100 beats per minute, with all beats being sinus-originated.

8. Sinus bradycardia: Heart rate below 60 beats per minute, with all beats being sinus-originated.

9. LVH: According to the Sokolow–Lyon index, this can be diagnosed when S wave amplitude in lead V1 plus R wave amplitude in lead V5 or V6 exceeds 35 mm, or the R wave amplitude in lead aVL exceeds 11 mm.

10. Left atrial overload: A widened P wave duration exceeding 0.12 seconds in leads I, II, and aVF, or an M-shaped or W-shaped P wave in lead V1.

11. LAFB: Left axis deviation (–45 to –90 degrees), QRS complex in lead I showing a dominant R wave, lead III showing a dominant S wave, and QRS duration less than 0.12 seconds.

12. RBBB: Presence of an rSR’ pattern in lead V1, with a QRS duration exceeding 0.12 seconds, and an S wave in leads I and V6 that is wider than the R wave.

13. VPBs: Broad and bizarre QRS complex, usually wider than 120 ms, with a discordant ST segment and T wave in relation to the QRS complex.

14. APBs: These are initiated by an aberrant P wave, which has a different morphology, axis, and timing than a normal sinus P wave. Typically, it is followed by a normal QRS complex.

15. AF: This is characterized by the absence of distinct P waves, replaced by irregular, rapid oscillations or fibrillatory waves. The ventricular response is irregular.

16. Degree I atrioventricular block: Every P wave is followed by a QRS complex, but

the PR interval is greater than 200 milliseconds (5 small squares).

Table S1. Comparison of the characteristics of All AD patients and Validation group AD patients

Variables	All AD (n = 313)	Validation group AD (n = 93)	*P*
Age, year, mean (SD)	59.1 (12.9)	59.2 (13.6)	0.94
Female, n (%)	58 (18.5)	12 (12.9)	0.27
Body temperature, mean (SD)	37.2 (0.8)	37.2 (0.8)	0.99
SBP (mm Hg), mean (SD)	142.2 (25.9)	144.9 (25.7)	0.38
DBP (mm Hg), mean (SD)	82.1 (17.2)	82.8 (17.0)	0.83
Diabetes, n (%)	176 (56.4)	50 (54.8)	0.73
Hypertension, n (%)	269 (85.9)	80 (86.0)	0.52
Smoke, n (%)	220 (70.3)	67 (72.0)	0.36
Alcohol, n (%)	223 (71.2)	63 (67.7)	0.42
Renal insufficiency, n (%)	212 (67.7)	63 (67.7)	0.91
Hyperlipidemia, n (%)	201 (64.4)	56 (60.9)	0.32
Hospital death, n (%)	17 (5.4)	4 (4.3)	0.12
D-dimer (μg/ml), median (IQR)	2.1 (1.0, 8.2)	1.8 (0.9, 5.7)	0.36
Creatinine (μgmol/l), median (IQR)	101.4 (28.2, 128.7)	98.2 (27.5, 102.7)	0.42
EGFR, ml/min/1.73 m², mean (SD)	74.9 (25.4)	71.7 (25.5)	0.29
CTn, ng/ml, median (IQR)	8.4 (3.6, 53.3)	8.6 (3.5, 66.3)	0.86
CRP, mg/l, median (IQR)	24.6 (5.2,29.7)	23.6 (4.8, 28.5)	0.54
PT, s, mean (SD)	14.5 (2.6)	14.4 (2.2)	0.74
Fbg, g/l, median (IQR)	3.1 (2.5, 4.0)	2.9 (2.5, 3.7)	0.62
APTT, s, mean (SD)	38.9 (15.2)	40.9 (20.0)	0.30
TT, s, median (IQR)	16.9 (15.8, 17.7)	17.2 (16.1, 18.0)	0.96

Compares characteristics between all AD patients (n = 313) and validation group AD (n = 93)
Abbreviations: APTT, activated partial thromboplastin time; CTn, cardiac troponin; CRP, C-reactive protein; DBP, diastolic blood pressure; EGFR, estimated glomerular filtration rate; Fbg, fibrinogen; PT, prothrombin time; SBP, systolic blood pressure; SD, standard deviation; TT, thrombin time
Values are mean (SD), n (%) or median (IQR)

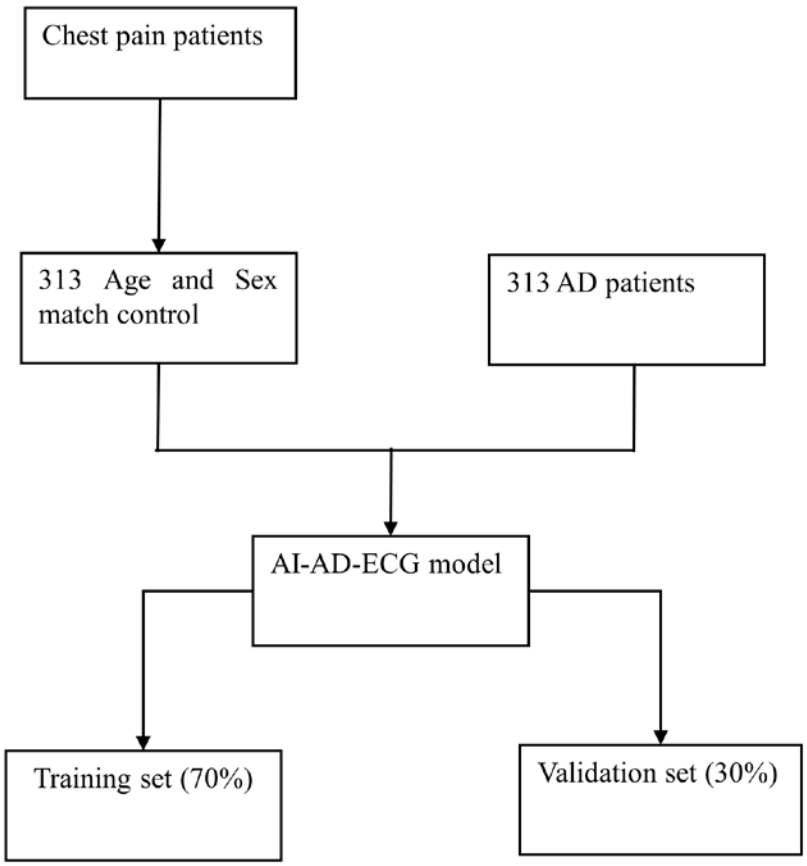

Figure S1. Study flowchart of special control group
Abbreviations: AD, aortic dissection; AI, artificial intelligence

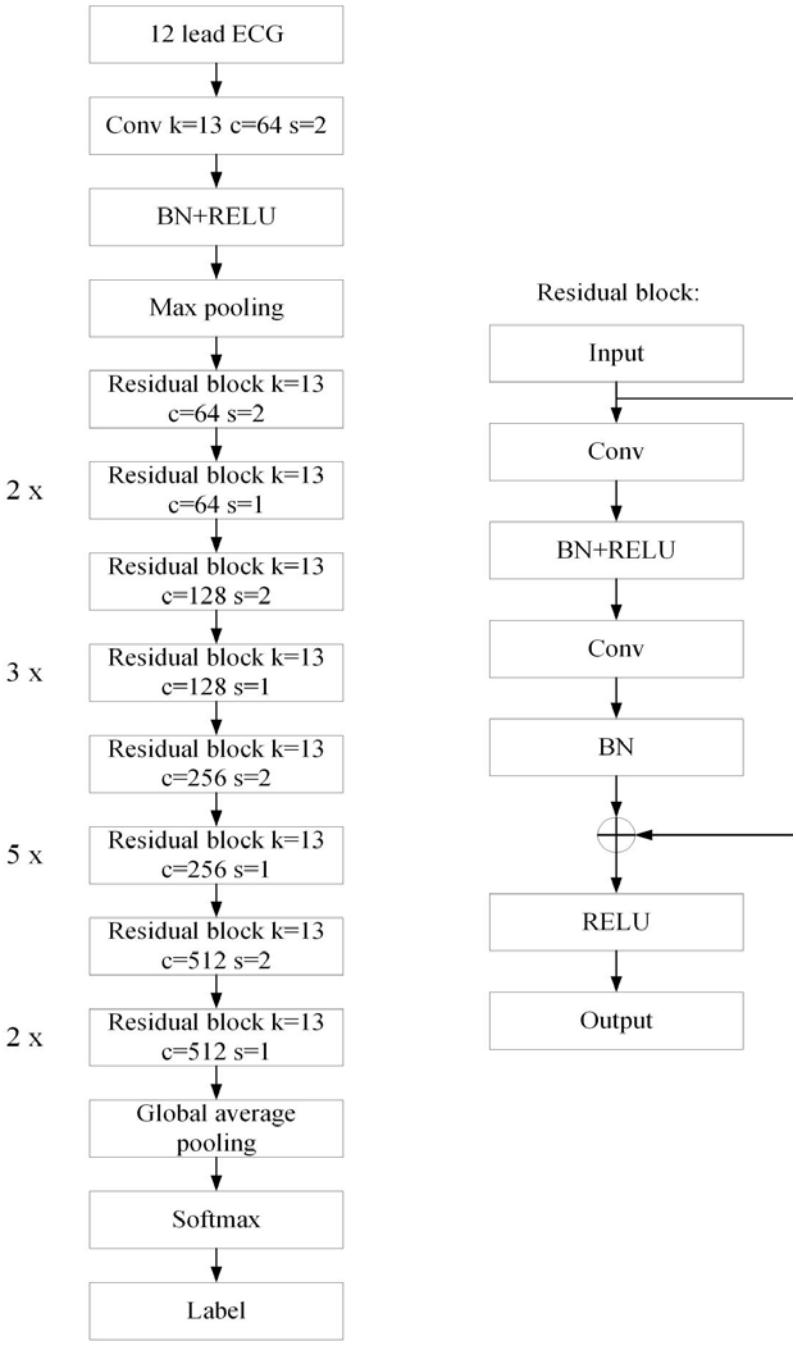

Figure S2. CNN architecture

Schematic representation of the proposed CNN architecture. The model was trained using 12-lead ECGs

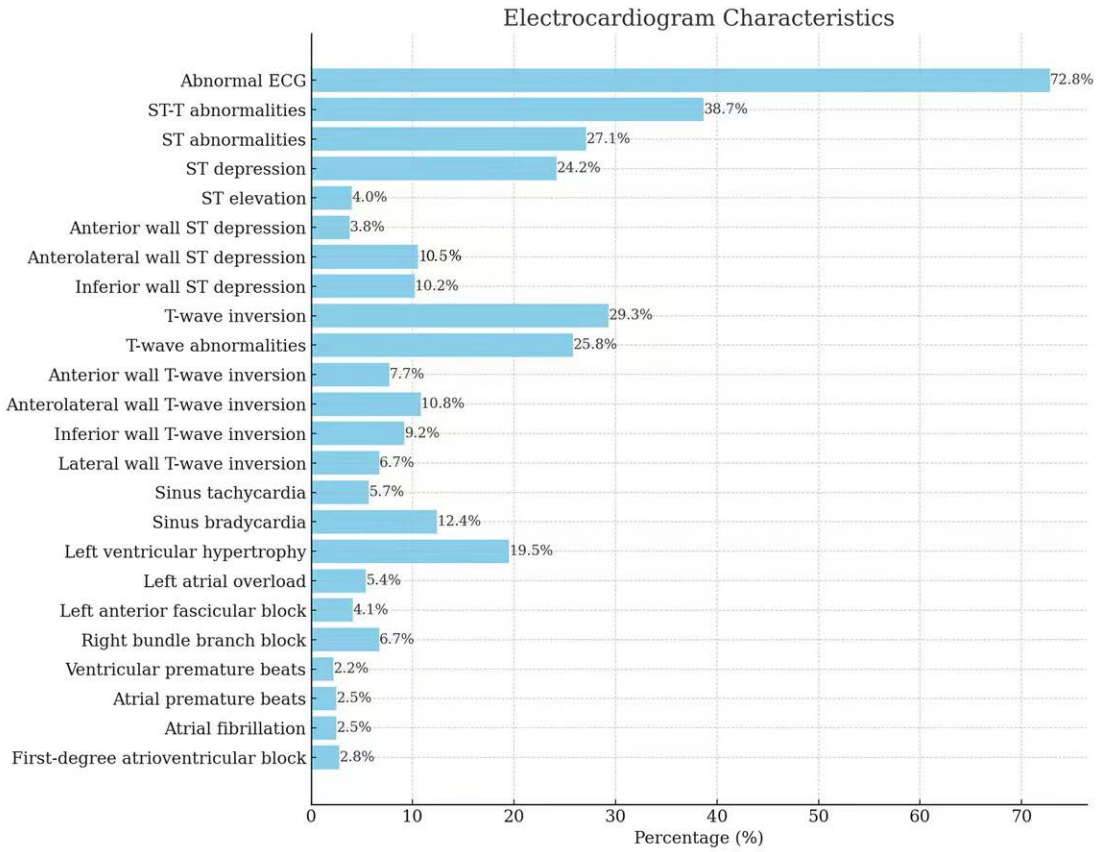

Figure S3. Electrocardiogram characteristics of 313 patients for AD

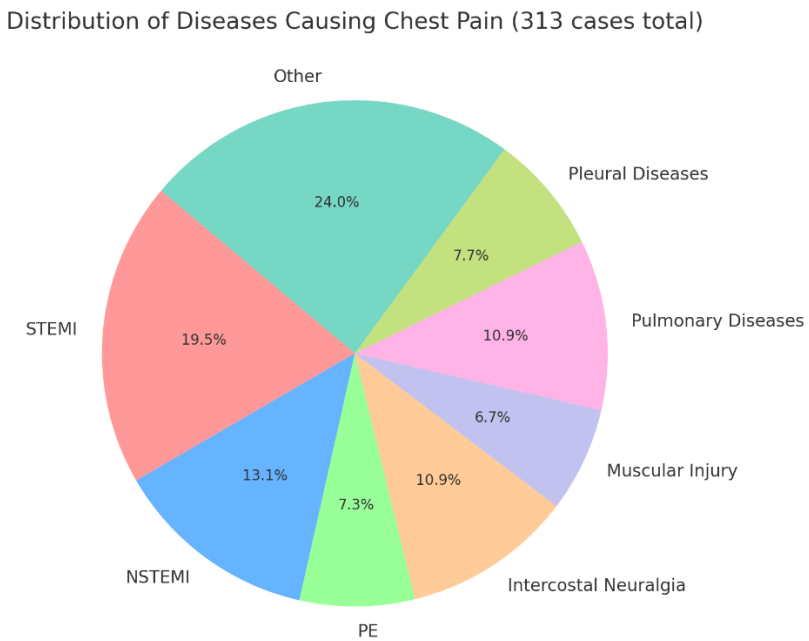

Figure S4. Distribution of diseases causing chest pain in special control group
Abbreviations: STEMI, ST-elevation myocardial infarction; NSTEMI, non-ST-elevation myocardial infarction; PE, pulmonary embolism

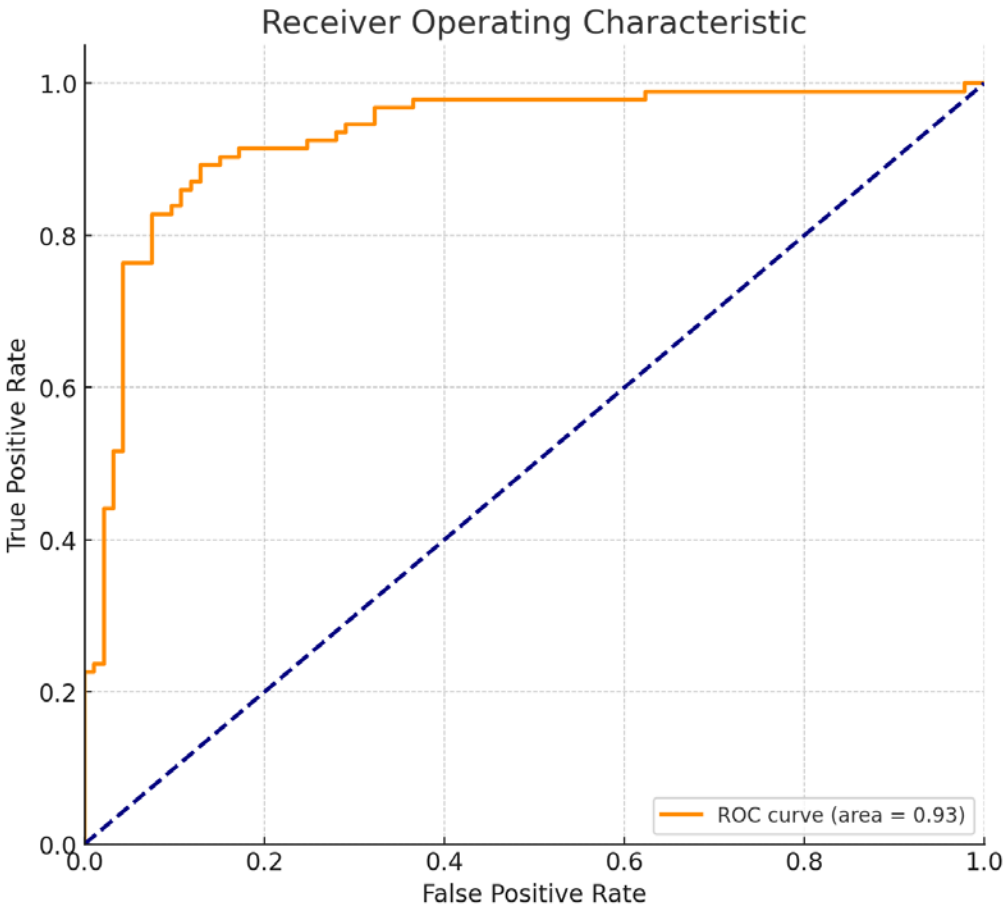

Accuracy	Sensitivity	Specificity	F1	AUC
0.871	0.839	0.903	0.871	0.928

Figure S5. Comparative performance of artificial intelligence algorithms in diagnosing aortic dissection among patients with chest pain

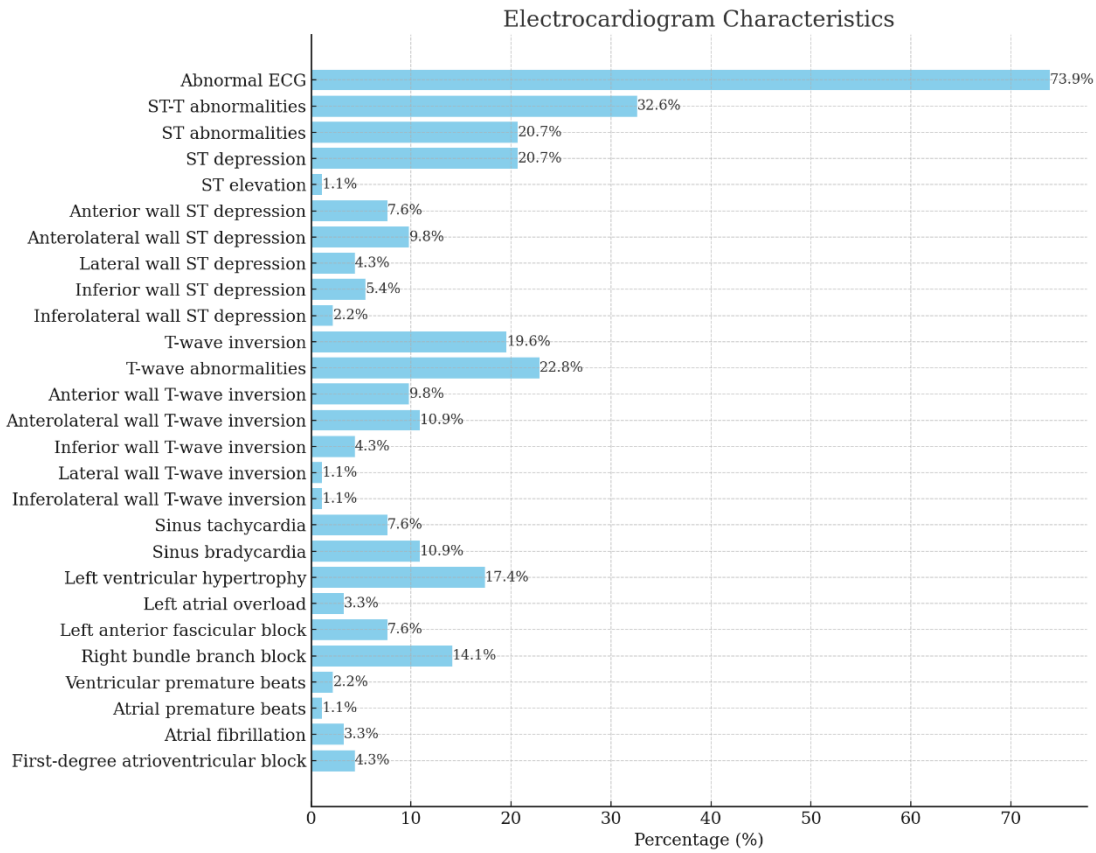

Figure S6. Electrocardiogram characteristics of 93 validation group patients